Polymer light emitting diodes and poly(di-*n*-octylfluorene) thin films as fabricated with a microfluidics applicator

H. Cheun
Materials Science Program, University of Wisconsin, Madison, Wisconsin 53706

P. P. Rugheimer[a]
Department of Physics, University of Wisconsin, Madison, Wisconsin 53706

B. J. Larson[b]
Materials Science Program, University of Wisconsin, Madison, Wisconsin 53706

P. Gopalan
Department of Materials Science and Engineering, University of Wisconsin, Madison, Wisconsin 53706

M. G. Lagally
Department of Physics, University of Wisconsin, Madison, Wisconsin 53706 and Department of Materials Science and Engineering, University of Wisconsin, Madison, Wisconsin 53706

M. J. Winokur[c]
Department of Physics, University of Wisconsin, Madison, Wisconsin 53706

A microfluidics applicator is used in the fabrication of a polyfluorene based polymer light emitting diode (PLED). This procedure results in a single contiguous polymer trace and, as a consequence of the high deposition speed, shows unusual characteristics in both the film morphology and polymer microstructure. These aspects are studied using fluorescence microscopy, profilometry, and optical absorption and emission spectroscopies. Room temperature analysis of the poly(di-*n*-octylfluorene) indicates that the combination of high-speed deposition and rapid drying process traps the polymer into a metastable conformational state. Optical spectroscopy at reduced temperature identifies emission from at least two distinct conformational chromophores. At elevated temperature there is an abrupt, irreversible transition to a more conventional structural form. Electroluminesence data from PLED test devices are shown and this demonstrates some of the unique opportunities afforded by this method of polymer film formation and device fabrication. Device operation is not optimized. © *2006 American Institute of Physics*. [DOI: 10.1063/1.2349467]

I. INTRODUCTION

In recent years organic semiconductors and conductors have undergone tremendous evolution and these materials are now proving competitive in a number of important device technologies.[1] Receiving particular emphasis are the π-conjugated polymers (CPs) and, depending on both chemical architecture and fabrication methods, a variety of applications have been developed including light emitting diodes,[2,3] transistors,[4] and photovoltaics.[5] Of these, conjugated polymer light emitting diodes (PLEDs) have seen major improvements since the seminal report of CP electroluminescence by Burroughes *et al.*[6]

Central for progress in these PLEDs and for CPs in general has been the development of techniques that control the physical state of the polymer and modify the surrounding environment. The recent literature abounds with reported fabrication methods and each has clear advantages and disadvantages.[7–12] Especially noteworthy is the use of ink-jet printing in which individual drops of a CP containing fluid are remotely targeted and arranged onto a substrate.[13] Although this approach is highly configurable and scalable, there are numerous caveats. For example, forming a single continuous linear trace by ink-jet printing necessarily requires the coalescence of multiple droplets. In this case the actual film morphology and microstructure may not have all the features necessary for optimal performance. Thus, as with any emerging technology, there is also a need to explore alternative methods for fabricating and testing device structures.

In this work we report on the use of a fluid microplotter for constructing CP based LEDs. This simple device dispenses fluid by using ultrasonic vibrations to move fluids in and out of the end of a micropipette reservoir.[14] By arranging for fluid contact with the surface and then moving either the tip or the substrate while maintaining this fluid contact, continuous features may be directly deposited onto a surface. The overall process itself is very well known and in many ways resembles the action of an old-fashioned fountain pen. Unlike ink-jet printing, which is a rigorously noncontacting method, or thermal transfer, in which the physical state of the CP is generally predefined, the fluid microplotter can potentially allow for *in situ* modification of the polymer films during the deposition process. Thus there are opportunities

---

[a]Present address: Physics Department, Montana State University, Bozeman, MT 59717.
[b]Present address: SonoPlot LLC, Madison, WI 53713.
[c]Electronic mail: mwinokour@wisc.edu

for exploiting shear and interfacial forces for manipulating both the film deposition and polymer microstructure.[15] The use of ultrasonics itself insures that multiple component fluids remain well mixed before and during deposition (although this aspect is not reported in this work). Finally, we note that commercial production of CP thin films will likely require high deposition speeds and, as such, the resultant films should reflect a highly nonequilibrium state.

This report therefore summarizes initial results for both film fabrication and PLED operation. We observe that the CP film properties are altered by even modest changes in the deposition conditions. There is overt impact to both the film surface morphology and the polymer microstructure. In particular, we can obtain flash evaporation of the solvent so that overlapping layers of different polymers are possible even when using a solvent common to both polymers. To characterize the resulting thin films we employ microscopy, spectroscopy, and profilometry. A simple working PLED is demonstrated but these properties have not as yet been optimized for real device applications.

II. EXPERIMENTAL DETAILS

A. Thin film deposition

Poly[9,9-(di-n,n-octylfluorene)] (PF8) was acquired from American Dye source and used as received. Unfiltered 1% and 2% w/w polymer/solvent solutions were prepared using chlorobenzene (CB). Other solvents were tried (e.g., toluene) but CB based solutions gave the best results in terms of observed trace repeatability and uniformity. All PF8 solutions were deposited onto planar sapphire substrates (ca. 100 μm thick), with nozzle linear speeds ranging from 100 to 3000 μm/s, by operating the microplotter in air under ambient conditions. Two specific solvent concentrations were tested, 1% and 2% w/w PF8/CB, and typical applicator test traces were 1 cm long and, depending on the applicator tip quality, 50–200 μm wide (as shown in Fig. 1). For base line comparison purposes 1% w/w solutions of PF8 in CB or toluene were either spin or drop cast. After deposition each individual test line was scanned cross ways (along the width) by profilometry using an Alphastep 200 Tencor Instrument. Fluorescence and polarization optical microscopies were also performed. After these measurements all samples were stored under vacuum and transferred onto a vacuum insulated oven/cryostat and then probed *in situ* using a custom built optical absorption (AB)/emission [AB/photoluminescence (PL)] spectrometer. Finally, a number of simple PLED devices were assembled and tested.

B. Light emitting diode fabrication

A schematic of the physical PLED layout is shown in Fig. 2. The substrate consisted of an etched indium tin oxide coated glass ($R=10\pm2$ Ω/sq) on top of which we deposited a thin layer of Bayer Baytron (PVP CH 8000) poly(ethyl-dioxythiophene) (PEDOT) by spin casting (at 6000 rpm). This layer was dried at 130 °C in a N$_2$ flushed oven.

To mask off all but a small area for use as a LED active device, we applied a poly(methylmethacrylate) (PMMA) insulating layer. This was accomplished by sequentially depos-
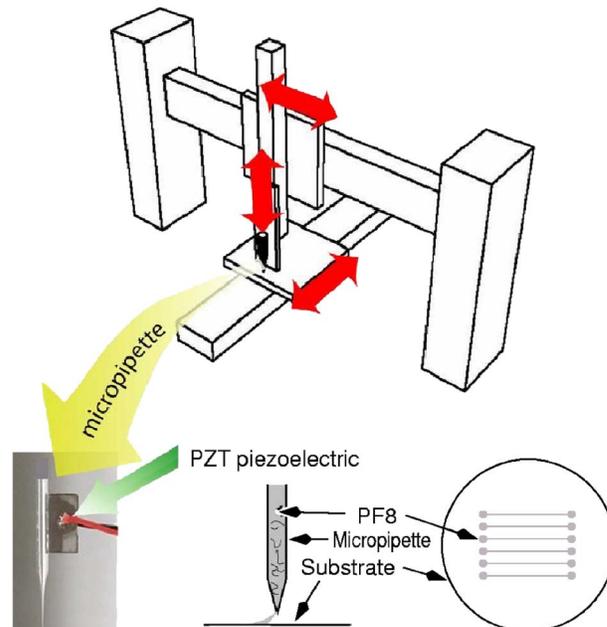

FIG. 1. (Color online) Top: schematic layout of the *XYZ* microplotter system that provides micron positional precision. Bottom: a photograph of the micropipette/piezoelectric crystal assembly and a typical test pattern of 1 cm long lines on the sapphire substrate.

iting multiple overlapping traces over the entire PEDOT surface except for (1) a thin PMMA free stripe exposing the PEDOT surface and (2) an open area for making electrical contact to the indium tin oxide (ITO). An active PF8 emitting layer was then deposited in the region not masked off by the PMMA traces at a deposition speed of 1000 μm/s using the 1% w/w PF8/CB solution. The test device was similarly dried in a N$_2$ flushed oven and then transferred into a thermal evaporator. The cathode of LED device was formed by sequentially depositing a Ca layer (ca. 8 nm) and then an Al metal cap (ca. 30 nm). All fabricated devices were mounted onto the same custom built dual AB/PL spectrometer. In this way both electroluminescence and PL emissions (not shown) could be monitored sequentially from the same location.

III. RESULTS AND DISCUSSION

A. Thin film deposition: Macromorphology

An important first step in the fabrication procedure was an overall assessment of the effect of high-speed film deposition. Recently Chen *et al.*[16] have reported that rapid drying of drop cast films[17] results in a significantly altered physical state in terms of PF8 emission. The action of this microplot-
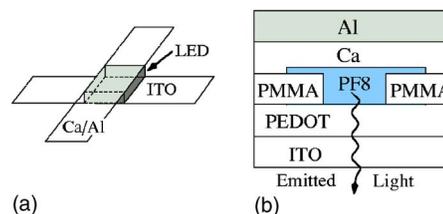

FIG. 2. (Color online) Schematic drawing of a working PF8 LED design as fabricated with the microplotter: (a) general spatial layout and (b) vertical layout.
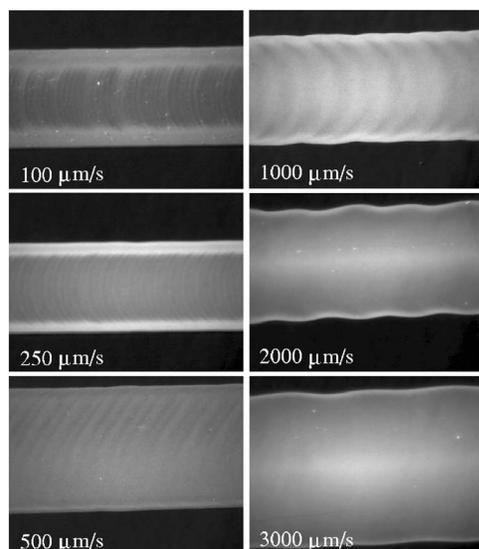
FIG. 3. Fluorescence microscopic images of individual microplotter traces at as indicated tip speeds.

FIG. 4. (Color online) Polarizing optical microscope images (at two magnifications) of a microplotter trace at the position of initial deposition.

ter is quite different than either ink-jet printing or thermal transfer. At a minimum the rapid movement of the micropipette tip at a position immediately above the substrate will produce high shear. The actual volume of deposited fluid at any one time is extremely small and thus the subsequent drying times are rapid. When monitoring this process through a video camera we observed a drying front that lagged close behind the applicator tip. The actual time between deposition and drying is estimated to occur in under 0.1 s at the highest applicator speeds although the precise moment at which a thin film is declared dry is clearly subjective.

The morphology of the film surface is also an essential attribute. Evaporation of the solvent from a deposited film is a highly nonequilibrium process that involves both the surface tension in the film and the solvent evaporation rate. Often the evaporation rate is greatest at the contact line where the solvent front ends.[8,18] This leads to a net flow of material towards this contact line and, in general, an increase in residual solute near the contact line. The process is commonly known as the "coffee ring" effect and results in a sharp rise of film thickness in the vicinity of the contact line.[19,20] In the case of ink-jet deposited films there can be negative consequences for PLED operation.

Films deposited by the microplotter were sensitive to both PF8 solution concentration and applicator speed. Selected fluorescence optical micrographs are shown in Fig. 3 and these demonstrate the gross morphological features. Quite evident is the repeating annulus pattern seen sequentially along the trace patterns at slower deposition speeds. We attribute this feature to the ultrasonic action of the applicator in which fluid rapidly flows in and out of the applicator tip. The exact solvent flow pattern was dependent on both the frequency and amplitude of the piezoelectric [lead zirconic titanate (PZT)] crystal. Variations in the texture of the deposited films indicate that this pattern forms at an average frequency of 1–10 Hz, a value much less than the actual PZT operating frequency. The net result was that films deposited
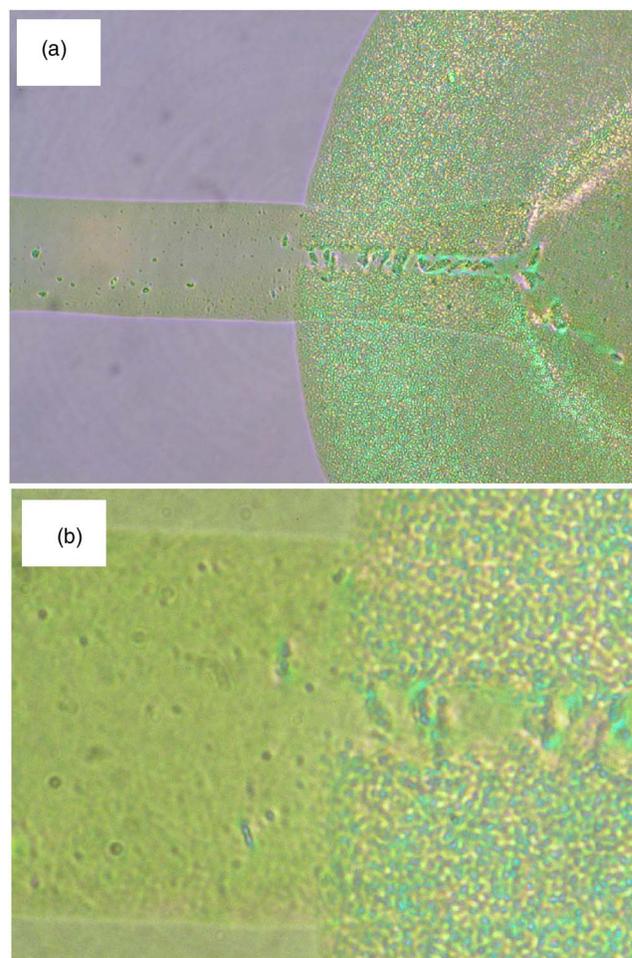
at the highest applicator translation speeds were generally the most uniform. In terms of obtaining an optimal film geometry both higher polymer concentrations and higher deposition speeds appear to be most desirable.

Many polyfluorene polymers are mesotropic and form liquid crystal (LC)-type phases.[16,21–23] Polarizing optical microscopy (POM) was used to assess this characteristic. POM images of all microplotter deposited films were typically uniform and nearly featureless regardless of deposition speed. Images positioned at the start of the linear motion resolve the morphological features of a small droplet residue in addition to those of the trace itself and are more revealing. An example of this, at two different magnifications, is shown in Fig. 4. After thermal cycling the droplet areas exhibit a classic Schlieren pattern indicative of a LC state whereas the linear test trace remains rather featureless. The droplet area retains inhomogeneities from the tip motion in addition to other aspects of the drying process.

Profilometry data, shown in Fig. 5, clearly demonstrate the wide variation in film height along the test trace cross sections. The coffee ring effect is most pronounced in films deposited at slower speeds and at lower PF8 concentrations. The 1% PF8/CB film deposited at 100 μm/s has a sharp rise of film thickness at the contact edge. Overall the film itself appears much thinner. This rise in thickness at the contact
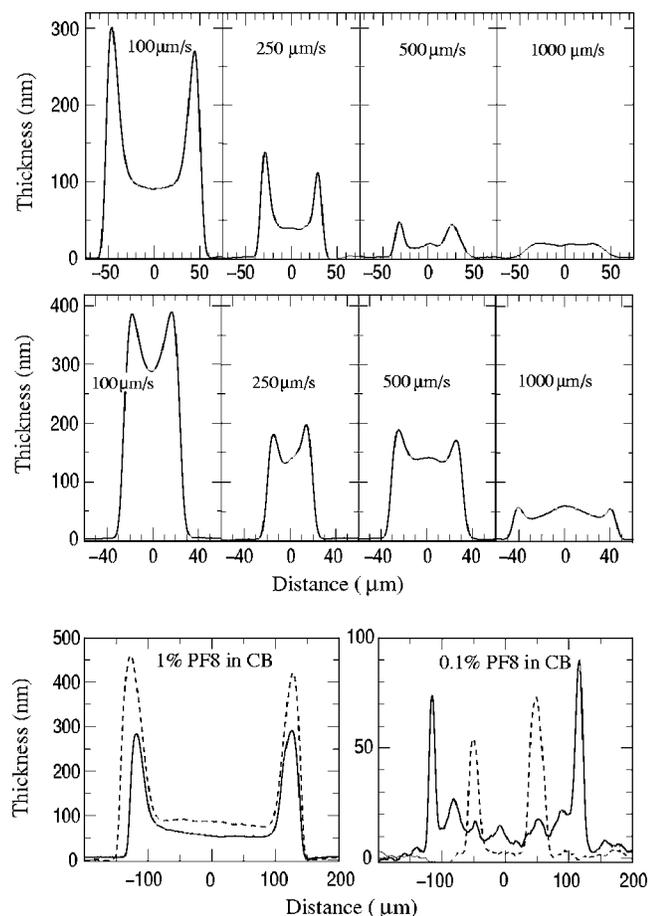
FIG. 5. Profilometer traces of PF8 thin film lines as fabricated by the microplotter at as indicated tip speeds. The widths range from 50 to 100 μm and the large rise in film thickness at the fluid contact line is most pronounced at low deposition speeds. Top: lines formed using 1% w/w PF8/CB solution. Middle: lines formed using 2% w/w PF8/CB solution. Bottom: Profilometer traces of PF8 thin films produced by drop casting from the indicated PF8/CB solutions.

line is almost entirely absent in lines formed at the highest deposition speeds. The net film thickness drops and these films approach 20–25 nm in net thickness. One interesting and reproducible feature is a secondary slow rise in the film thickness halfway across the profilometer trace. This small rise is most apparent at the highest tip deposition speeds. This feature can also be distinguished in the fluorescence micrographs as a bright emission ridge along the center of the trace. There is at least one report in the literature that discusses droplet drying modes[24] and the appearance, in circular droplets, of a "Mexican hat" shape. Our observed behavior may be the consequence of this effect in combination with the one-dimensional translational movement of the stylus.

For comparison purposes Fig. 5 also displays profilometry data from a few drop cast films. When using a 1% PF8/CB solution it proved difficult to prepare drops much smaller than 200 μm in diameter. In addition the net film thicknesses were typically higher than those using the applicator. The height at the contact line is proportionately larger as well. Drop casting from toluene solutions gave poor results and so these data are not shown. To achieve thinner film thicknesses and smaller overall dimensions we also tried a

0.1% w/w PF8/CB solution and two example drop cast film traces are shown in the right bottom panel of Fig. 5. In this case the relative thickness rise at the contact line is quite pronounced. In addition many of the larger diameter drops displayed a rippling surface profile indicative of secondary drying instabilities. In general the droplet to droplet variation was quite large.

B. Microstructure and spectroscopy

Not only is the film surface morphology sensitive to the explicit forming conditions but also the polymer microstructure itself is measurably altered by the deposition conditions. This can be clearly discerned in steady state emission spectroscopy. To provide proper background we note that even among polyfluorenes PF8 is known to be especially polymorphic in terms of both the single chain morphology and interchain packing.[22] Thin film measurements resolve singlet exciton emission (i.e., from prompt fluorescence) signatures indicative of up to three distinct emitting chromophores.[22,25–28] Recently Chunwachirasiri *et al.*[29] have proposed a molecular level model in which there are differentiated families of conformational isomers. These are designated as C_α-, C_β- and C_γ-type conformers. The most unusual of these is the so called C_β type (or β phase and reported in a large number of publications[30–32]) and this low energy absorption band is attributed to isolated chain segments of enhanced local order and increased intrachain fluorene-fluorene planarity. There is additional evidence that the β phase is metastable in thin films.[27] Also observed is, depending on the solvent and film casting conditions, a broad low energy emission band. This feature may be attributed to either interchain excitations[33] or chemical defects.[34]

In most instances the photoluminescence from PF8 films cast from toluene, *p*-xylene, chlorobenzene, and similar solvents is wholly dominated by β phase emission. A typical example of this (from a PF8/toluene spin cast film) is shown in Figs. 6(a) and 6(b) at both reduced temperature (70 K) and at near room temperature (290 K). (Photoluminescence from our drop cast films was essentially identical to that of the spin cast film except for the occurrence of self-absorption effects at emission energies above 2.75 eV.) At 290 K the direct π^*-π transition [or zero phonon line (ZPL)] is centered near 2.83 eV and, at lower energy, there is a series of vibronic replicas representing the manifold of local vibrational modes of the PF8 polymer.[30,31,35] The 2.83 eV centered peak also includes contributions from a superposition of low energy vibronic modes. Reduced temperature results in a measurable narrowing of these singlet exciton emission features and, additionally, reduces the proportion of the broadband emission background. The β phase emission becomes exceptionally well resolved (for a polymer). Also included in Figs. 6(a) and 6(b) are direct fits of the observed PL to the full Franck-Condon (FC) expression using the same methodology as reported in Refs. 29 and 36. The background profile (thin dashed line) reflects both the broadband emission feature and a possible breakdown of the FC formula (which assumes simple Poisson statistics for the higher order vibronic terms).
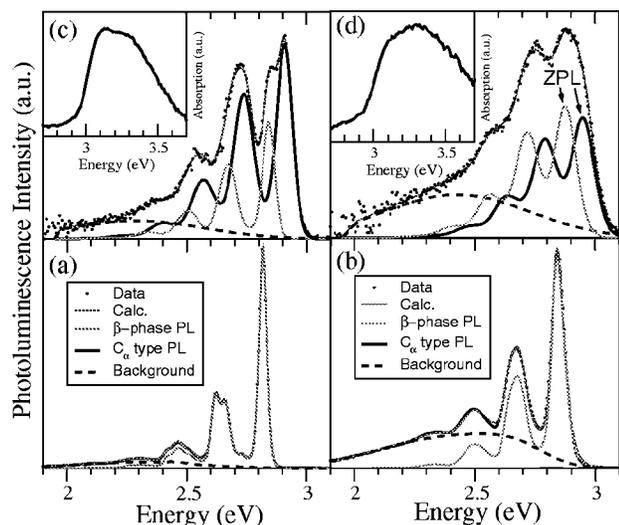
FIG. 6. (Color online) Franck-Condon analysis of PL data (see text for details) from [(a) and (b)] conventional spin cast films (from a 1% w/w PF8/toluene solution) at 70 and 290 K, respectively, assuming that emission originating from β phase chains superimposes on a broad background (black dashed line). [(c) and (d)] Film deposited at 1000 μm/s (from 2% w/w PF8/CB solution) assuming that emission originates from a superposition the β phase (lower energy ZPL, green), C_α segments (higher energy ZPL, blue), and a broad background (black dashed line) at 80 K (c) and at 303 K (d).
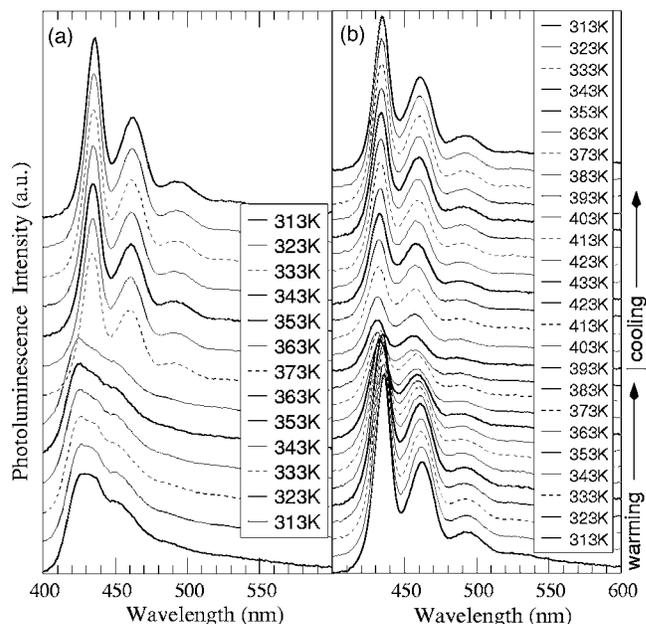

FIG. 7. Temperature dependent PL spectra from film deposited at 1000 μm/s (from 2% w/w PF8/CB solution) on thermal cycling: (a) from 313 K (bottom) up to 373 K (middle) and back down to 313 K (top); (b) same film on second thermal cycle from 313 K (bottom) up to 433 K (middle) and back down to 313 K. All spectra have been offset and rescaled for clarity.

Figures 6(c) and 6(d) display typical PL and AB spectra from a 100×300 μm^2 section of a single line trace after deposition at 1000 μm/s using the 2% w/w PF8/CB solution. These spectra are significantly different than those of Figs. 6(a) and 6(b) (i.e., reflective of a β phase dominated film). Lower deposition speeds, typically at 250 μm/s or less, typically yield PL spectra that contain a large fraction of β phase emission. As the deposition speed increases the relative proportion of β phase emission drops. The room temperature scan, in Fig. 6(d), is qualitatively similar to that seen by Chen *et al.*[16] (after rapid drying of a drop cast film using a blowing stream of nitrogen gas). The apparent relative drop in the ZPL emission in comparison with that seen in the vibronic overtones is suggestive of a net increase in the electron-phonon coupling (or, equivalently, the Huang-Rhys parameters). Rapid deposition presumably causes a substantial increase in the level of disorder. This produces an overall decreases in the effective conjugation length and consequently a net blueshift in both the center peak position of the ZPL and those of the of vibronic subbands.

Although the room temperature line shape gives the naive appearance of being comprised by a single broad emitting chromophore, these flash dried PF8 film data actually evidence emission by a short wavelength chromophore in superposition with that of the β phase. This attribute is impossible to discern near room temperature but becomes self-evident on cooling to 80 K, a temperature at which the respective emission peaks have narrowed. At 80 K this β phase emission is resolved as a pronounced shoulder at 2.84 eV superimposed on a somewhat broader emission band centered at higher energy. In terms of the photoabsorption (see the respective insets) there is no distinct low energy absorption feature and so the actual proportion of β phase sites must be very small.

A FC analysis of the PL data from the applicator drawn traces can be conducted by superimposing a second FC progression on that of the original β phase progression and broad background. The resulting fits are also shown in Figs. 5(c) and 5(d). The component originating from β phase emission is broader than that of the spin cast sample shown in Fig. 5(a). The high energy emission band (centered at 2.95 eV) is broader still and most resembles PL from C_α-type conformers.[29] This latter attribute is consistent with formation of a spin cast glass.

Even when analyzed as separately resolved FC profiles one can observe the anomalous strength of the vibronic replicas at low energy (i.e., below 2.8 eV). The relative intensity of these FC subbands (0–1, 0–2, and so on) is clearly larger that that of the β phase dominated spin cast film and, in reference to Ref. 29, those of samples dominated by emission from other conformational isomers (C_α or C_γ type). In regard to LED device applications this trend towards very broad emission bands will ultimately affect the color purity. Hence there may be secondary device performance consequences that arise as the CP field pushes towards higher speed deposition methods for increased throughput.

The thermal stability of the films formed by these high-speed depositions is also an interesting topic. The optical properties of these films were examined during thermal cycling to elevated temperatures and thermal cycling eventually leads to irreversible change in the PL emission spectra. Two example sequences are shown in Fig. 7 for a stripe deposited at 1000 μm/s. Upon heating the PL continues to broaden and the vibronic subbands become even less well defined. Part of this effect can be attributed to disordering of the β phase (at ca. 350 K). However, at temperatures just
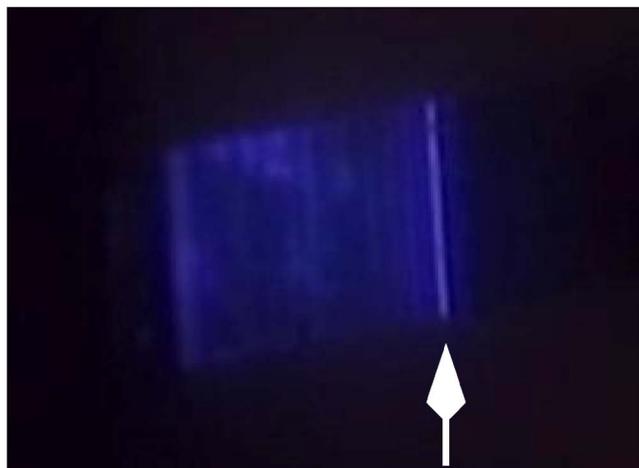
FIG. 8. (Color online) Example of blue light emission from PF8 PLED fabricated with the microplotter. The image is slightly distorted by the 45° rotation of the PLED substrate with respect to the CCD viewing camera. (Color scale, online version, is not accurate.)

FIG. 9. Example electroluminescence spectra from two different PLED devices operated at the indicated voltages.

above 363 K the PL profile in Fig. 7(a) undergoes a sudden change that includes a rapid rise in the emission normal to the film surface. By 373 K there is a very well defined FC vibronic progression with the ZPL centered near 435 nm. The β phase is not stable at these temperatures and so this emission is presumed to reflect yet another conformational isomer. The mostly likely candidate is the claimed C_γ family of conformational isomers. For spin cast or drop cast films the transition to this state generally occurs at somewhat higher temperatures.[27] A second thermal heating/cooling cycle of the interconverted film, shown in Fig. 7(b), primarily produces a monotonic drop in the emission intensity (on heating) with only a partial recovery of the emission intensity on cooling. Scans of the other applicator deposited films are qualitatively similar.

The sudden increase in the observed emission at ca. 365 K during the first heating cycling may be due to overt changes in PF8 properties at the molecular level or, alternatively, a irreversible alteration in the surface morphology with the development of planar waveguiding.[37] Because the film surface is initially very smooth at the onset it seems that this effect is not a major factor but rather change at the molecular level is a more likely culprit. Still we note that Ariu *et al.*[38] have examined similar temperature ranges in spin cast PF8 films and do not identify sudden large variations in the PL quantum yield. Directional changes in the molecular level chain orientation with respect to the substrate are also a distinct possibility. The specific underlying mechanism responsible for this behavior is still unknown.

C. Light emitting diode

Finally, we comment on PLED test device emission properties. In these devices the plotter was used to apply both the passive PMMA mask and the active PF8 layer. An example of the emission from a working polymer LED device is shown in Fig. 8. This particular device exhibited turn on at an applied bias voltage of 4 V. The blue emission seen here actually originates from the thin vertical strip (40 μm
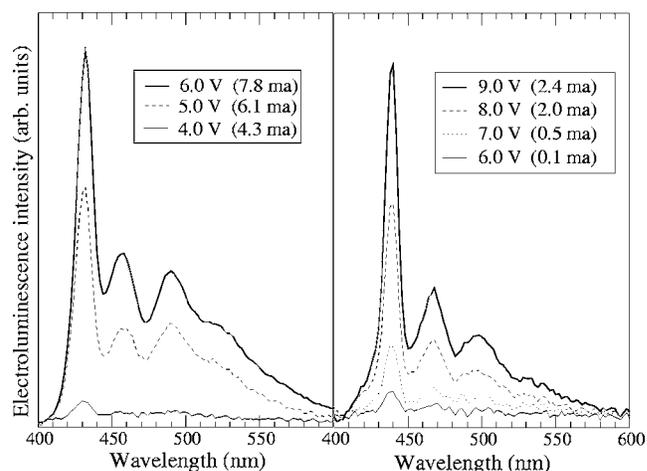
×1 mm) on the right as indicated by the white arrow. However, there also appears to be waveguiding into to the PMMA mask region and, because of inhomogeneities, this light is partially scattered out the top. The lifetime of the working devices was relatively short (only a few hours) but this aspect was not optimized in any way.

Sample electroluminescence (EL) spectra from two different devices are shown in Fig. 9. The first has its ZPL emission peaked at 432 nm while the second is slightly blue-shifted to 438 nm. There are also some slight voltage dependent variations in the EL line shapes. The spectra on left include a greater proportion of the often seen broadband emission but in all other ways the two devices are similar. The relative proportion of aggregate emission is greater in these EL spectra as compared to that seen in the PL spectra. This is a common result that is often attributed to differences in the exciton recombination zone between PL and EL. PL of thin films generally reflects the entire sample whereas EL often is dominated by light emission originating close to the cathode. The latter is attributed to higher hole mobilities in comparison with those of electrons.[39]

IV. CONCLUSIONS

The utility of using an ultrasonic micropipette deposition systems in the construction of polymer LEDs has been demonstrated. High-speed deposition of thin films promotes flash freezing of these polymers and, in reference to PF8, suppresses formation of the β phase even when using good solvents with a relatively low vapor pressure. These films also include an increased level of conformational disorder but, at least for PF8, this can be eliminated by thermal annealing. In terms of real-world applications this methodology does not appear to be scalable for large scale production. However, operation of this device at high deposition speeds produces a single smooth continuous trace with a very well defined surface morphology. In its current form this methodology has merit for producing well controlled polymer thin films in the design and testing of prototype devices. As such we expect that the microplotter deposition method will also prove useful in polymer field-effect transistor studies.

ACKNOWLEDGMENTS

[1] S. R. Forrest, Nature (London) **428**, 918 (2004).

[2] J. Burroughes, C. Jones, and R. Friend, Nature (London) **335**, 1684 (1988).

[3] H. Sirringhaus, N. Tessler, and R. H. Friend, Science **280**, 1741 (1998).

[4] C. Dimitrakopoulos and D. Mascaro, IBM J. Res. Dev. **45**, 12 (2001).

[5] C. J. Brabec, N. S. Sariciftci, and J. C. Hummelen, Adv. Funct. Mater. **11**, 26 (2001).

[6] J. J. Burroughes, D. D. C. Bradley, A. R. Brown, R. N. Markes, K. Mackay, R. H. Friend, P. L. Burns, and A. B. Holmes, Nature (London) **347**, 539 (1990).

[7] T. Kawase, T. Shimoda, C. Newsome, H. Sirringhaus, and R. H. Friend, Thin Solid Films **438**, 279 (2003).

[8] B. J. de Gans and U. S. Schubert, Langmuir **20**, 7789 (2004).

[9] L. J. Guo, J. Phys. D **37**, R123 (2004).

[10] T. W. Lee, J. Zaumseil, Z. N. Bao, J. W. P. Hsu, and J. A. Rogers, Proc. Natl. Acad. Sci. U.S.A. **101**, 429 (2004).

[11] P. C. Kao *et al.*, IEEE Trans. Electron Devices **52**, 1722 (2005).

[12] K. Cheng, M. H. Yang, W. W. W. Chiu, C. Y. Huang, J. Chang, T. F. Ying, and Y. Yang, Macromol. Rapid Commun. **26**, 247 (2005).

[13] B. J. de Gans, P. C. Duineveld, and U. S. Schubert, Adv. Mater. (Weinheim, Ger.) **16**, 203 (2004).

[14] B. J. Larson, S. D. Gillmor, and M. G. Lagally, Rev. Sci. Instrum. **75**, 832 (2004).

[15] S. C. Bae, Z. Q. Lin, and S. Granick, Macromolecules **38**, 9275 (2005).

[16] S. H. Chen, A. C. Su, and S. A. Chen, J. Phys. Chem. B **109**, 10067 (2005).

[17] Chen *et al.* use only toluene in their study whereas chlorobenzene, used in our work, has a much lower vapor pressure and is hence more difficult to effect a "rapid" drying.

[18] J. Buehrle, H. Sirringhaus, and F. Mugele, Langmuir **18**, 9771 (2002).

[19] R. D. Deegan, O. Bakajin, T. F. Dupont, G. Huber, S. R. Nagel, and T. A. Witten, Nature (London) **389**, 827 (1997).

[20] X. J. Wang, M. Ostblom, T. Johansson, and O. Inganäs, Thin Solid Films **449**, 125 (2004).

[21] M. Grell, D. D. C. Bradley, X. Long, T. Chamberlain, M. Inbasekaran, and E. P. Woo, Acta Polym. **49**, 439 (1998).

[22] M. Grell, D. D. C. Bradley, G. Ungar, J. Hill, and K. S. Whitehead, Macromolecules **32**, 5810 (1999).

[23] S. H. Chen, A. C. Su, C. H. Su, and S. A. Chen, Macromolecules **38**, 379 (2004).

[24] L. Pauchard and C. Allain, Phys. Rev. E **68**, 052801 (2003).

[25] A. J. Cadby *et al.*, Phys. Rev. B **62**, 15604 (2000).

[26] A. J. Cadby, P. A. Lane, M. Wohlgenannt, C. An, Z. V. Vardeny, and D. D. C. Bradley, Synth. Met. **111**, 515 (2000).

[27] H. Cheun, B. Tanto, W. Chunwachirasiri, B. Larson, and M. J. Winokur, Appl. Phys. Lett. **84**, 22 (2004).

[28] A. L. T. Khan, P. Sreearunothai, L. M. Herz, M. J. Banach, and A. Köhler, Phys. Rev. B **69**, 085201 (2004).

[29] W. Chunwachirasiri, B. Tanto, D. L. Huber, and M. J. Winokur, Phys. Rev. Lett. **94**, 107402 (2005).

[30] M. Ariu *et al.*, Phys. Rev. B **67**, 195333 (2003).

[31] M. J. Winokur, J. Slinker, and D. L. Huber, Phys. Rev. B **67**, 184106 (2003).

[32] S. H. Chen, H. L. Chou, A. C. Su, and S. A. Chen, Macromolecules **37**, 6833 (2004).

[33] V. N. Bliznyuk, S. A. Carter, J. C. Scott, G. Klaerner, R. D. Miller, and D. C. Miller, Macromolecules **32**, 361 (1999).

[34] E. J. W. List, R. Guentner, P. S. de Freitas, and U. Scherf, Adv. Mater. (Weinheim, Ger.) **14**, 374 (2002).

[35] J. Teetsov and M. A. Fox, J. Mater. Chem. **9**, 2117 (1999).

[36] J. Gierschner, H. G. Mack, L. Luer, and D. Oelkrug, J. Chem. Phys. **116**, 8596 (2002).

[37] M. Sims, K. Zheng, M. Campoy Quiles, R. Xia, P. N. Stavrinou, D. D. C. Bradley, and P. Etchegoin, J. Phys.: Condens. Matter **17**, 6307 (2005).

[38] M. Ariu, D. G. Lidzey, M. Sims, A. J. Cadby, P. A. Lane, and D. D. C. Bradley, J. Phys.: Condens. Matter **14**, 9975 (2002).

[39] D. Neher, Macromol. Rapid Commun. **22**, 1366 (2001).